SMiRT-12 / K. Kussmaul (Editor)

K09/2

UNCERTAINTY OF RESTORING FORCE CHARACTERISTICS OF SHEAR WALLS AND ITS EFFECT ON SEISMIC RESPONSE

Y. Kai[1], M. Takeda[1], R. Shohara[1], K. Ohtani[2] and K. Akino[3]

[1]Shimizu Corp., Tokyo, [2]National Research Institute for Earth Science and Disaster Prevention, Tukuba, [3]Nuclear Power Engineering Corp., Tokyo (Japan)

1. Introduction

Study on advanced seismic design for LWR has been carried out by the Nuclear Power Engineering Corporation (NUPEC), under the sponsorship of the Ministry of International Trade and Industry (MITI) of Japan. This paper describes the uncertainty of the restoring force characteristics of a shear wall based on the existing static loading test data of box wall and cylindrical wall specimens. The effect of the uncertainty of the restoring force characteristics on the dynamic response is also studied using a single-degree-of-freedom(SDOF) system.

2. Statistic analysis of restoring force characteristics of shear walls

The envelope curves are idealized with tri-linear models as shown in Fig. 1. The equations for the location of each intersection are summarized on Table 1. The uncertainty of envelope curves of each specimen is modeled by the coefficients a ~ d.

The load-displacement hysteresis loops are idealized with a pair of three-degree functions as shown in Fig. 2. The coefficient B is determined by the gradient at zero displacement. The coefficient A is determined by the equivalent damping h_E. Therefore, the uncertainty of load-displacement hysteresis loop is modeled by two parameters, which are the coefficient B and the equivalent damping h_E

Table 2 shows the list of the test specimens used in this statistic analysis. The sample size is 43. The specimens are classified into two categories, which are the box wall type (box wall, I-shape wall) and the cylindrical wall type (diagonal loading of box wall, octagonal tube wall, cylindrical wall). Among these specimens, the hysteresis data are measured only in 20 specimens.

Table 3 shows the result of the statistical analysis of the test data. The mean stress levels of the first and second intersections and the maximum point are as same as the calculated values by the equations. The maximum displacement of the test result is larger than the value of the equation. This is because that the equation for the maximum displacement is aimed to predict the lower limit of the allowable deformation. The coefficients of variance (c.o.v.) of each parameter are 20%, except the c.o.v. of the maximum displacement is 30%. The mean value and the c.o.v. of the equivalent damping are 5 ~ 6% abd about 20% respectively. The mean value and the c.o.v. of the coefficient B is 0.6 ~ 0.7 and about 40% respectively. Table 3 also shows the correlation factors of each parameter.

3. Response analysis of SDOF system considering the uncertainty of the restoring force characteristics

To study the effect of the uncertainty of the restoring force characteristics on the dynamic response, Monte Carlo simulation analysis is carried out using SDOF system considering the variation of the restoring force characteristics and the input motion. The parameters of the analysis are the resonant period, the configuration of the wall, the characteristics of hysteresis loops and the plasticity level. The analysis cases are summarized on Table 4. For each case, 100 Monte Carlo samples are generated considering the statistic characteristics studied in the previous section. The correlation of each parameter is also taken into account. The maximum stress level is determined from the linear response to the design basis earthquake S_1 (M7, Δ20km, phase El Centro, maximum acceleration 267.4gal). The mean of the maximum stress level is set into 2 levels based on this design stress. In one case, the mean of the maximum stress is set equal to the design stress level. In the other case, the mean of the maximum stress level is set as three-times of the design stress level.

Ten ground motion data are used as the sample of the input motion. The statistic characteristics of these waves are shown in Fig. 3. The maximum accelerations of each ground motion data are normalized to 267.4gal that is as same level as the maximum acceleration of the design basis earthquake S_1.

Table 5 shows the statistical results of the dynamic response analyses of Monte Carlo samples. Each value is compared with the linear response analysis results. The c.o.v. of the linear response result is about 25 ~ 45 %. This variation is due to the variation of the input motion. The mean value of each result in the non-linear analysis, when the maximum stress level is set to three-times of the design stress level, is almost as same values as the linear analysis results. The c.o.v. of the response shear stress and the maximum acceleration in the non-linear analysis, however, becomes smaller than the linear analysis result. The mean of the ductility factor (maximum strain / cracking strain) in this case is about 0.8 ~ 0.95.

The means of the shear stress and the maximum acceleration in the non-linear analysis are 50 ~ 70 % of those obtained from the linear analysis in the case that the maximum stress level is set equal to the design stress level. The c.o.v. of the shear stress and the maximum acceleration in the non-linear analysis is about 20 %, which is much smaller than the linear analysis result. On the other hand, the mean and the c.o.v. of the shear strain in the non-linear analysis are larger than the linear analysis result.

To see the effect of the hysteresis rule, Table 5 also compares the result using the three-degree function type and the peak-oriented type hysteresis rule. In the three-degree function type hysteresis rule, the uncertainty of the hysteresis loop besides the uncertainty of the envelope curve is considered. In the peak-oriented type hysteresis rule, however, the uncertainty of the envelope curve is only considered. The statistical result shows that the mean and the c.o.v. of the shear stress and strain become smaller when the three-degree function type rule is used.

Table 5 also compares the difference of response due to the wall configuration. The mean and the c.o.v. of all response of the box wall except the shear strain are larger than those of the cylindrical wall.

The c.o.v. of each response also differs among the cases with the different resonant periods. In the linear analysis, the c.o.v. is smallest for the case that the resonant period T = 0.2 sec. In the non-linear analysis, the order of the c.o.v. of the velocity and the shear strain among the system with the different resonant period is as same order as in the linear analysis. The c.o.v. of the maximum acceleration and the shear stress,however, is almost same despite the difference of the resonant period in the non-linear analysis.

Table 6 shows the ratio of the stresses in the non-linear analysis and the linear analysis, and the ductility factor. In general, the ratio of the stresses in the non-linear analysis and the linear analysis becomes smaller when the ductility factor becomes larger because of much plastic energy absorption. In the system with resonant period T=0.1sec, however, even though the ductility factor is larger, the ratio of the stresses is larger than the results in the systems with resonant period t=0.2sec. and 0.3sec. The peak of the response spectrum of the input motion is around 0.2sec. For the system with the resonant period T=0.1sec., the effective energy input becomes larger when the effective resonant period becomes longer due to the plastic response of the system. The c.o.v. of the ratio of the stresses in the non-linear analysis and the linear analysis keep constant even when their mean values are different. The c.o.v. of the ductility factor becomes larger as the mean value of ductility factor becomes larger. The ratio of the stresses in the non-linear analysis and the linear analysis calculated from the response using the peak-oriented type hysteresis rule is larger than the result using the three-degree function type hysteresis rule. The ductility factor and the ratio of the stresses in the non-linear analysis and the linear analysis of box wall are larger than those of cylindrical wall.

4. Conclusion

The uncertainty of the restoring force characteristics is evaluated from the existing test data. Using the Monte Carlo simulation analysis considering the uncertainty of restoring force characteristics and input motion, the variation of response force is found to be 20 % in the non-linear response.

Acknowledgments

This work was carried out by NUPEC as the entrusted project sponsored by the Ministry of International Trade and Industry in Japan. This work was supported by "Committee on advanced seismic design for LWR" of NUPEC. The authors wish to express their gratitude for the cooperation and valuable suggestion given by the members of the Committee.

References

[1]Umemura, H. et al. (1976), Experimental study on capacity and restoring force characteristics of RC shear walls, the Proceeding of Kanto branch of AIJ (in Japanese)
[2]Nagashima, H. et al. (1979), Report on the horizontal load test of cylindrical RC walls, the Proceeding of Kansai branch of AIJ (in Japanese)
[3]Yano, A. et al. (1985), Experimental study on the mechanics of joint of large bar, the Summaries of technical papers of AIJ annual meeting (in Japanese)
[4]Endo, A. et al. (1985), Experimental study on the kinematic property of box wall under 2 directional force, the Summaries of technical papers of AIJ annual meeting (in Japanese)
[5]Akino, K. et al. (1982), Restoring force characteristics test of nuclear power plant, the Summaries of technical papers of AIJ annual meeting (in Japanese)
[6]Joint Research Study (1985), Study of cost reduction using high strength rebar and concrete, the intermediate report of first half year of 1985 (in Japanese)
[7]Nuclear Power Engineering Test Center (1984), Restoring force characteristics test of nuclear power plant -- scale effect test, the Annual report of 1983 (in Japanese)

Table 1 Equation of Each Point of Envelope Curve

$(\gamma_1, \tau_1) \sim (\gamma_3, \tau_3)$:location of intersection		$\tau_0=(3.0-1.8\times M/QD)\sqrt{F_c}$ $(M/QD\le 1.0)$
$\tau_1=\sqrt{\sqrt{F_c}\times(\sqrt{F_c}+\sigma_V)}$	$\gamma_1=\tau_1/G$	$\tau_S=(P_V+P_H)s\sigma_y/2+(\sigma_V+\sigma_H)/2$
$\tau_2=1.35\tau_1$	$\gamma_2=3\gamma_1$	F_c : compress strength of concrete (kgf/cm2)
$\tau_3=\left[1-\tau_S/(4.5\sqrt{F_c})\right]\tau_0+\tau_s$	$\gamma_3=4.0\times10^{-3}$	G : shear modulus of concrete (kgf/cm2)
$(\text{if } \tau_S\le 4.5\sqrt{F_c})$		P_V, P_H : vertical, horizontal rebar ratio
$=4.5\sqrt{F_c}\ (\text{if } \tau_S\ge 4.5\sqrt{F_c})$		σ_V, σ_H : vertical, horisontal axial stress (positive in compression) (kgf/cm2)
		$s\sigma_y$:yield stress of the rebar (kgf/cm2)
		M/QD : shear span ratio

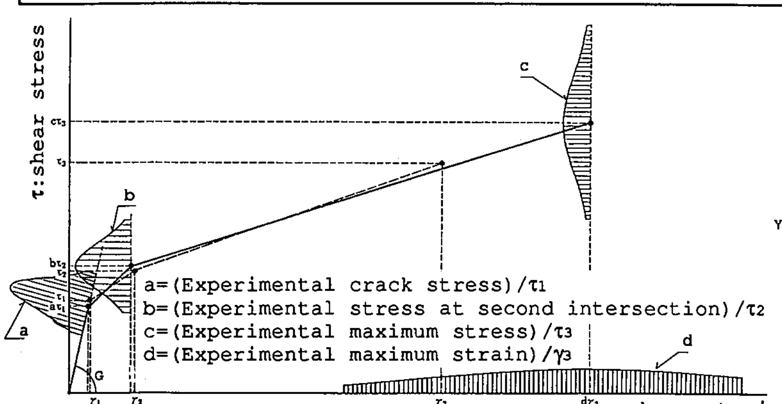

Fig.1 Envelope Curve

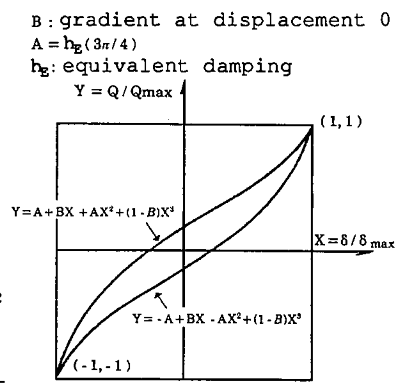

Fig.2 Hysteresis Loop

Table 2 Test Specimens

specimen	configure	height of loading point(cm)	depth of loading slab(cm)	section parameters: web depth (cm)	section parameters: flange width(cm)	section parameters: wall thick-ness(cm²)	shear span ratio	area of web (cm²)	rebar ratio: P_V (%)	rebar ratio: P_H (%)	axial stress (kg/cm²)	Fc* (kg/cm²)	cE* ×10⁵ (kg/cm²)	diameter of aggregates(mm)	sσy* (kg/cm²)	sE* ×10⁶ (kg/cm²)	ref.
TUB-10R	B	80.0	10.0	75.0	75.0	8.0	1.07	1200.0	1.60	1.00	0.0	231	2.12	15	3906	****	
TUB-16	B	80.0	10.0	75.0	75.0	8.0	1.07	1200.0	1.60	1.60	0.0	190	2.55	15	3906	****	1
TUC-30	C	80.0	10.0	75.0	-	10.0	1.07	1178.0	3.00	3.00	0.0	175	1.63	15	3929	****	
C25A1-24	C	120.0	10.0	114.0	-	6.0	1.05	1074.5	2.40	1.20	0.0	242	1.97	10	3310	****	2
LSDHE-01	I	190.0	40.0	239.0	119.0	39.0	0.80	9321.0	1.63	1.63	0.0	229	2.47	25	3887	1.91	3
LSDHE-02	I	190.0	40.0	239.0	119.0	39.0	0.80	9321.0	1.63	1.63	0.0	313	2.18	25	3887	1.91	
TWDNO.1	B	90.0	30.0	150.0	150.0	8.0	0.60	2400.0	1.20	1.20	20.0	382	2.38	10	4465	1.99	
TWDNO.2	B	90.0	30.0	150.0	150.0	8.0	0.60	2400.0	1.20	1.20	20.0	228	1.48	10	4465	1.99	4
TWDNO.3	B	90.0	30.0	150.0	150.0	8.0	0.60	2400.0	1.20	1.20	0.0	304	2.76	10	4544	1.99	
B1-1	B	60.0	30.0	150.0	150.0	8.0	0.40	2400.0	0.80	0.80	20.0	277	2.43	10	3840	1.87	
B1-2	B	60.0	30.0	150.0	150.0	8.0	0.40	2400.0	1.20	1.20	0.0	247	2.25	10	3840	1.87	
B1-3	B	120.0	30.0	150.0	150.0	8.0	0.80	2400.0	0.80	0.80	20.0	248	2.20	10	3840	1.87	
B1-4	B	120.0	30.0	150.0	150.0	8.0	0.80	2400.0	1.20	1.20	0.0	305	2.29	10	3840	1.87	
B1-5	B	120.0	30.0	150.0	150.0	8.0	0.80	2400.0	1.20	1.20	20.0	297	2.68	10	3840	1.87	
B1-6	B	120.0	30.0	150.0	150.0	16.0	0.80	4800.0	1.20	1.20	0.0	275	2.18	10	3750	1.71	
B1-7	B	120.0	30.0	150.0	150.0	8.0	0.80	2400.0	1.60	1.60	0.0	247	2.15	10	3840	1.87	
B2-1	C	60.0	20.0	100.0	-	8.0	0.60	1256.5	0.76	0.80	0.0	283	2.54	10	3840	1.87	
B2-2	C	60.0	20.0	100.0	-	8.0	0.60	1256.5	1.53	1.60	0.0	277	2.48	10	3840	1.87	
B2-3	C	60.0	20.0	100.0	-	8.0	0.60	1256.5	1.53	1.60	20.0	275	2.45	10	3840	1.87	5
P1-1	C	120.0	40.0	142.0	-	8.0	0.85	1784.0	1.61	1.61	0.0	271	1.91	15	3840	1.87	
P1-2	D	120.0	40.0	158.3	-	8.0	0.76	1792.0	1.57	1.57	0.0	257	1.78	15	3840	1.87	
P1-3	O	120.0	40.0	134.2	-	8.0	0.89	1788.0	1.51	1.51	0.0	247	2.02	15	3840	1.87	
P1-4	O	120.0	40.0	134.2	-	8.0	0.89	1788.0	1.51	1.51	0.0	253	1.77	15	3840	1.87	
P1-5	O	120.0	40.0	134.2	-	8.0	0.89	1788.0	1.51	1.51	0.0	286	2.04	15	3840	1.87	
P1-6	O	120.0	40.0	134.2	-	8.0	0.89	1788.0	1.51	1.51	0.0	228	1.84	15	3840	1.87	
P1-7	O	120.0	40.0	134.2	-	8.0	0.89	1788.0	0.75	0.75	0.0	221	1.74	15	3840	1.87	
P1-8	O	120.0	40.0	134.2	-	8.0	0.89	1788.0	2.29	2.29	0.0	241	1.79	15	3840	1.87	
P1-P	O	120.0	40.0	134.2		8.0	0.89	1788.0	1.51	1.51	0.0	206	1.66	15	3840	1.87	
P2-4	O	78.0	22.0	93.0	-	19.0	0.84	2930.0	2.00	2.00	0.0	235	1.86	15	4670	1.87	
W-12-1	I	100.0	50.0	200.0	50.0	12.0	0.50	2400.0	1.32	1.32	20.0	359	2.69	20	3790	1.79	
W-12-2	I	100.0	50.0	200.0	50.0	12.0	0.50	2400.0	0.90	0.90	20.0	387	2.54	20	3790	1.79	
W-12-3	I	100.0	50.0	200.0	50.0	12.0	0.50	2400.0	1.69	1.69	20.0	365	2.51	20	3790	1.79	
W-12-4	I	100.0	50.0	200.0	50.0	12.0	0.50	2400.0	1.32	1.32	10.0	365	2.58	20	3790	1.79	
W-12-5	I	100.0	50.0	200.0	50.0	12.0	0.50	2400.0	1.32	1.32	20.0	348	2.48	20	3790	1.79	6
W-12-6	I	200.0	50.0	200.0	50.0	12.0	1.00	2400.0	1.32	1.32	10.0	338	2.51	20	3790	1.79	
W-12-7	I	200.0	50.0	200.0	50.0	12.0	1.00	2400.0	1.32	1.32	10.0	346	2.43	20	3790	1.79	
W-15-1	I	100.0	50.0	200.0	50.0	15.0	0.50	3000.0	1.06	1.06	20.0	253	2.17	20	3790	1.79	
W-15-2	I	200.0	50.0	200.0	50.0	15.0	1.00	3000.0	1.06	1.06	20.0	264	2.27	20	3790	1.79	
S-1	I	120.0	20.0	150.0	83.0	8.0	0.80	1200.0	1.60	1.60	0.0	304	2.56	10	4021	1.86	
S-2	I	360.0	60.0	450.0	249.0	24.0	0.80	10800.0	1.60	1.60	0.0	234	2.08	25	3980	1.91	
S-3	I	360.0	60.0	450.0	249.0	24.0	0.80	10800.0	1.60	1.60	0.0	263	2.27	25	4014	1.94	7
S-4	I	360.0	60.0	450.0	249.0	24.0	0.80	10800.0	1.60	1.60	0.0	231	2.26	10	3980	1.91	
S-5	I	360.0	60.0	450.0	249.0	24.0	0.80	10800.0	1.60	1.60	0.0	253	2.10	10	4010	1.94	

*configuration marks; B:box wall, D:diagonal loading of box wall, O:octagonal tube wall, C:cylindrical wall, I:I-shape wall
*Pv,PH:vertical and horizontal rebar ratio of the wall respectively
*Fc, cE, sσy, sE:data from test peace, ****:unknown
*sample size:43, 20 specimens shown in the ref. 5 had the data of hysteresis loops

Table 3 Statistical result of test specimens

configuration		box wall						cylindrical wall					
parameters		a	b	c	d	h_E(%)	B	a	b	c	d	h_E(%)	B
sample size		28				14		15				26	
mean		0.98	1.03	1.18	1.40	5.07	0.67	0.92	0.90	0.99	2.38	6.19	0.57
standard deviation		0.17	0.19	0.21	0.44	0.80	0.26	0.23	0.16	0.10	0.77	1.31	0.16
correlation factor matrix	a	1.00	0.03	-0.03	-0.09	-0.02	-0.34	1.00	0.80	0.45	-0.36	-0.67	0.28
	b	0.03	1.00	0.24	-0.22	-0.13	0.65	0.80	1.00	0.59	-0.48	-0.74	0.37
	c	-0.03	0.24	1.00	0.70	0.38	0.42	0.45	0.59	1.00	-0.54	-0.66	0.49
	d	-0.09	-0.22	0.70	1.00	0.63	-0.70	-0.36	-0.48	-0.54	1.00	0.26	-0.24
	h_E	-0.02	-0.13	0.38	0.63	1.00	-0.27	-0.67	-0.74	-0.66	0.26	1.00	-0.20
	B	-0.34	0.65	0.42	-0.70	-0.27	1.00	0.28	0.37	0.49	-0.24	-0.20	1.00

Table 4 Analysis Cases

CASE NO.	configuration: cylinder	configuration: box	resonance period (sec) T=0.1	T=0.2	T=0.3	(mean maximum stress)/(design stress) 1.0	3.0	hysteresis: peak oriented	hysteresis: 3-degree function
1	●		●			●		●	
2	●		●			●			●
3	●			●		●		●	
4	●			●		●			●
5	●				●	●		●	
6	●				●	●			●
7		●	●			●		●	
8		●		●		●		●	
9		●			●	●		●	
10	●		●				●	●	
11	●		●				●		●
12		●	●				●	●	

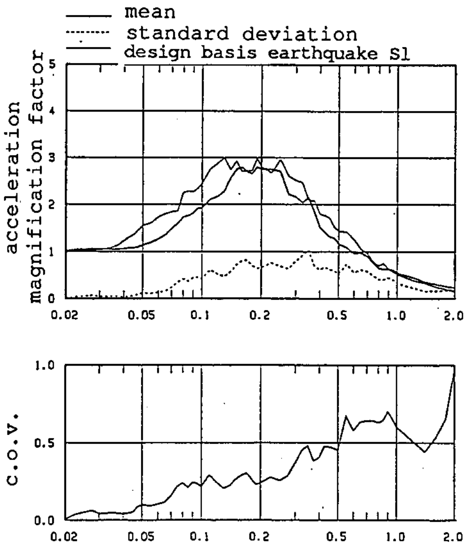

Fig.3 Statistic Characteristics of Input Waves

Table 5(1) Statistical Result of Response Analysis (maximum stress/design stress)=1.0

response	response period(sec)	cylinder	box	3-degree function	peak oriented	linear analysis m* (cov*)	non-linear analysis mean m	m/m*	c.o.v. cov	cov/cov*
acceleration (gal)	T=0.1	○		○			403.4	0.637	0.144	0.433
		○			○	633.3	413.0	0.652	0.199	0.612
			○		○	(0.325)	458.9	0.725	0.218	0.671
	T=0.2	○		○			419.5	0.500	0.169	0.663
		○			○	838.2	436.9	0.521	0.172	0.675
			○		○	(0.255)	462.8	0.552	0.214	0.839
	T=0.3	○		○			311.7	0.450	0.171	0.378
		○			○	692.6	332.5	0.480	0.174	0.385
			○		○	(0.452)	351.9	0.508	0.192	0.425
velocity (kine)	T=0.1	○		○			12.491	1.517	0.426	1.231
		○			○	8.234	13.788	1.675	0.508	1.468
			○		○	(0.346)	14.132	1.716	0.515	1.488
	T=0.2	○		○			19.670	0.783	0.288	1.134
		○			○	25.137	23.615	0.939	0.259	1.020
			○		○	(0.254)	24.470	0.973	0.304	1.197
	T=0.3	○		○			21.229	0.651	0.312	0.770
		○			○	32.586	25.933	0.796	0.343	0.847
			○		○	(0.405)	26.579	0.816	0.353	0.872
shear stress (kgf/cm^2)	T=0.1	○		○		54.72(cyl)	33.73	0.616	0.148	0.460
		○			○	65.22(box)	34.43	0.629	0.198	0.615
			○		○	(0.323)	46.42	0.712	0.213	0.659
	T=0.2	○		○		60.08(cyl)	29.41	0.490	0.168	0.661
		○			○	71.61(box)	30.59	0.509	0.175	0.689
			○		○	(0.254)	39.04	0.545	0.212	0.835
	T=0.3	○		○		62.38(cyl)	27.44	0.440	0.169	0.371
		○			○	74.35(box)	29.19	0.468	0.168	0.369
			○		○	(0.455)	37.12	0.499	0.187	0.411
shear strain (×0.0001)	T=0.1	○		○		4.975(cyl)	17.014	3.42	0.642	1.988
		○			○	5.930(box)	17.429	3.503	0.681	2.108
			○		○	(0.323)	19.561	3.299	0.664	2.056
	T=0.2	○		○		5.462(cyl)	6.802	1.245	0.475	1.870
		○			○	6.511(box)	7.897	1.446	0.433	1.705
			○		○	(0.254)	9.335	1.434	0.466	1.835
	T=0.3	○		○		5.671(cyl)	5.160	0.910	0.535	1.176
		○			○	6.760(box)	6.405	1.129	0.568	1.248
			○		○	(0.455)	7.761	1.148	0.566	1.244

Table 5(2) Statistical Result of Response Analysis (maximum stress/design stress)=3.0 resonance period T=0.1sec

response	cylinder	box	3-degree function	peak oriented	linear analysis m* (cov*)	non-linear analysis mean m	m/m*	c.o.v. cov	cov/cov*
acceleration (gal)	○		○			596.3	0.942	0.261	0.803
	○			○	633.3	605.2	0.956	0.259	0.797
		○		○	(0.325)	590.6	0.933	0.220	0.677
velocity (kine)	○		○			7.853	0.954	0.313	0.905
	○			○	8.234	8.247	1.002	0.330	0.954
		○		○	(0.346)	8.289	1.007	0.338	0.977
shear stress (kgf/cm^2)	○		○		18.24(cyl)	17.20	0.943	0.261	0.808
	○			○	21.74(box)	17.49	0.959	0.259	0.802
		○		○	(0.323)	20.37	0.937	0.222	0.687
shear strain (×0.0001)	○		○		1.658(cyl)	1.617	0.975	0.283	0.876
	○			○	1.976(box)	1.683	1.015	0.331	1.025
		○		○	(0.323)	2.031	1.028	0.351	1.087

Table 6 Ductility Factor and Ratio of the Stresses in the Non-linear Analysis and the Linear Analysis

	response period(sec)	(maximum stress/design stress) 1.0: cylinder, 3-d	1.0: cylinder, peak oriented	1.0: box, peak oriented	3.0: cylinder, 3-d	3.0: cylinder, peak oriented	3.0: box, peak oriented
ratio of the stresses in the non-linear analysis and the linear analysis	T=0.1	0.655 (0.275)	0.673 (0.272)	0.757 (0.257)	0.959 (0.098)	0.973 (0.072)	0.958 (0.086)
	T=0.2	0.516 (0.270)	0.537 (0.282)	0.564 (0.220)	-	-	-
	T=0.3	0.511 (0.390)	0.539 (0.361)	0.571 (0.355)	-	-	-
ductility factor	T=0.1	9.963 (0.848)	9.219 (0.822)	9.402 (0.704)	0.807 (0.401)	0.825 (0.446)	0.954 (0.455)
	T=0.2	3.610 (0.585)	4.142 (0.552)	4.524 (0.515)	-	-	-
	T=0.3	2.702 (0.651)	3.147 (0.568)	3.723 (0.598)	-	-	-

note;upper data:mean, lower data in parenthesis:c.o.v.